PHYSICAL REVIEW B VOLUME 48, NUMBER 15 15 OCTOBER 1993-I

Surface-plasmon dispersion and size dependence of Mie resonance: Silver versus simple metals

A. Liebsch
Institut für Festkörperforschung, Forschungszentrum, 517 Jülich, Germany
(Received 18 September 1992; revised manuscript received 27 April 1993)

The recently observed blueshift of the surface plasmon of Ag with increasing parallel momentum and of the Mie resonance of small Ag particles with decreasing radius are discussed in terms of a model for the dynamical response of a two-component *s-d* electron system. In the case of flat Ag surfaces, the 5*s* conduction electrons are treated as a semi-infinite homogeneous electron gas while the influence of the fully occupied 4*d* bands is described via a polarizable medium which extends up to a certain distance from the surface. Using the time-dependent density-functional approach it is shown that the absence of the *s-d* screening interaction in the surface region leads to a positive dispersion of the surface plasmon in agreement with the data. A self-energy approach is introduced which allows us to establish a qualitative relation between the scattering processes at a flat metal surface and those at the surface of a spherical particle. Using this approach it is argued that the blueshift of the Mie resonance of Ag particles can also be understood in terms of a reduced *s-d* interaction in the region where the *s* electrons spill out into the vacuum. Finally, it is shown that the polarizability of simple metal particles exhibits above the Mie resonance a collective excitation which is the analogue of the dipolar surface plasmon observed on the flat surfaces of various simple metals. This feature seems to have been observed in recent absorption spectra on large K clusters.

I. INTRODUCTION

Electron-energy-loss measurements on all low-index crystal faces of Ag have recently shown[1-3] that the surface plasmon disperses towards higher frequencies with increasing parallel momentum. This positive dispersion is in striking contrast to the behavior of the ordinary surface plasmons on all simple metals (Al, Na, K, Cs) (Refs. 4 and 5) which show a negative dispersion at small wave vectors. This initial negative slope is a direct consequence of the fact that the centroid of the fluctuating charge associated with the surface plasmon of a simple metal is located outside the nominal metal surface.[6,7] Similarly, the Mie resonance in optical-absorption spectra from small Ag particles was recently observed to shift to higher frequencies with decreasing particle size.[8-11] Again, this blueshift is opposite to the redshift that is seen for the Mie resonance of small simple metal particles.[12,13] The redshift in the latter case is related to the so-called spill-out effect, i.e., to the fact that, just as on the flat surface, the centroid of the charge fluctuation associated with the Mie resonance is located outside the particle surface. The important conclusion from these data is, therefore, that the presence of the Ag 4*d* electrons influences, in a fundamental manner, the mechanism that determines the initial dispersion of the surface plasmon and the size dependence of the Mie resonance.

In principle, the 4*d* band of Ag can affect the dynamical surface response in two distinct ways: First, the *s-d* hybridization modifies the single-particle energies and wave functions. As a result, the nonlocal density-density response function exhibits band-structure effects. Second, the effective time-varying fields are modified due to the mutual polarization of the *s* and *d* electron densities. In the present work we focus on the role of the second mechanism for the following reason: At the parallel wave vectors of interest, the frequency of the Ag surface plasmon lies below the region of interband transitions involving the filled 4*d* states or higher-lying unoccupied *s-p* states which begin at about 3.9 eV. Thus, the single-particle transitions that contribute to the collective surface excitations all occur within the *s-p* band close to the Fermi energy where it displays excellent nearly free-electron character. The interband transitions enter therefore only as virtual transitions and should not play the principal role that governs the wave-vector dispersion of the Ag surface plasmon. Since these virtual transitions depend on the surface band structure, their effect should be different for various crystal faces. Thus, these transitions are presumably responsible for the fact that the slopes of the surface plasmons differ for the three low-index faces of Ag.[1-3] The common positive dispersion on all of these faces, on the other hand, i.e., the fundamental sign reversal compared to the dispersion found for the simple metals, is apparently caused by a more basic mechanism that modifies the intraband transitions within the nearly-free-electron *s-p* band.

Similar arguments can be made for the size dependence of the Ag Mie resonance since its frequency lies even lower than that of the Ag surface plasmons. Thus, the relevant single-particle transitions that contribute to the Mie collective mode primarily involve states that have *s-p* character similar to those in simple metal particles. Transitions involving the more tightly bound *d* levels, on the other hand, can contribute only in a virtual fashion and should therefore not play the most important role for the size dependence of the Mie resonance.

The main goal of this paper is to show that the second mechanism mentioned above, namely, the mutual polarization between the Ag 5*s* and 4*d* states, does indeed have

0163-1829/93/48(15)/11317(12)/$06.00 ©1993 The American Physical Society

a significant effect on the dispersion of the collective surface modes of Ag and that this mechanism is the main physical origin of the observed positive dispersion of the Ag surface plasmon and of the Ag Mie resonance. Essentially, the $5s$ and $4d$ electrons will be treated as a two-component system whose electrostatic interaction extends only up to a certain distance from the surface. In particular, this interaction is absent in the region where the $5s$ electron density spills out into the vacuum. Since the electrons oscillate in this region with the unscreened plasma frequency, this mechanism causes an increase of the surface-plasmon frequency. This effect becomes more important with increasing parallel wave vector and with decreasing particle radius because of the greater relative weight of the surface region. As a result, both the surface-plasma frequency and the Mie resonance exhibit a positive dispersion with increasing momentum and with decreasing radius, respectively.

It is well known that in the bulk the s-d polarization is responsible for the large renormalization of the Ag volume plasma frequency. This may be seen as follows:[14] The volume dielectric properties of Ag can be qualitatively represented by a Drude term $\epsilon_s(\omega)$ appropriate for the $5s$ electrons and a "bound" contribution $\epsilon_d(\omega)$ whose frequency dependence is primarily governed by the interband transitions from the occupied $4d$ band to the $5s$ conduction bands near the Fermi level. Thus, the measured dielectric function can be decomposed as $\epsilon(\omega) = \epsilon_s(\omega) + \epsilon_d(\omega) - 1$. Near to the region of the collective modes of Ag, $\epsilon_d(\omega)$ is real and has a value of about 5 to 6. As a result of this bound term, the volume plasma frequency is reduced from the unscreened value, $\omega_p = 9.2$ eV, to the observed value which is approximately given by $\omega_p^* \approx \omega_p / \sqrt{\mathrm{Re}\epsilon_d} \approx 3.76$ eV. Accordingly, the frequency of the surface plasmon in the long-wavelength limit is given by $\omega_s^* \approx \omega_p / \sqrt{1 + \mathrm{Re}\epsilon_d} \approx 3.64$ eV whereas the unscreened value is $\omega_s = \omega_p / \sqrt{2} = 6.5$ eV. Similarly, the frequency of the Mie resonance in the large particle limit is given by $\omega_M^* \approx \omega_p / \sqrt{2 + \mathrm{Re}\epsilon_d} \approx 3.50$ eV whereas the unscreened value is $\omega_M = \omega_p / \sqrt{3} = 5.3$ eV. As will be shown below, the renormalization of these surface collective modes due to the mutual s-d polarization is less pronounced at finite parallel wave vectors or at finite particle radii because of the spillout of the $5s$ electrons into the vacuum.

The dynamical response calculations for the model discussed above will be carried out in detail for the case of the surface-plasmon dispersion on flat Ag surfaces. In order to evaluate the surface excitation spectra we use the time-dependent local-density approximation[15] (TDLDA) which has led to an excellent overall description of the dispersion of both the ordinary monopole surface plasmon and of the so-called multipole surface plasmon for various simple metals (Al, Na, K, Cs).[4,5] In principle, the same model could be applied also to determine the absorption spectrum of small Ag particles. This calculation would require the same computational effort as the evaluation of the absorption cross section of jellium particles. In order to simplify this step, we first rewrite the surface response function at small q by introducing an effective local dielectric function which involves a complex surface self-energy. This self-energy accounts for the quantum-mechanical scattering processes occurring in the surface region. The shift and finite width of the surface plasmon are directly related to the real and imaginary parts of this self-energy, respectively. Since these scattering events typically occur within a thin region of the dimension of an electronic screening length, we then assume that the self-energy processes at the surface of a spherical particle in the limit of large radii are similar to those at a flat metal surface in the long-wavelength limit. On the basis of this analogy we can express the complex particle polarizability in terms of a corresponding self-energy which determines the shift and broadening of the classical Mie resonance. These arguments show that the blueshift of the Ag Mie resonance with decreasing radius has the same physical origin as the blueshift of the Ag surface plasma frequency with increasing parallel momentum.

An additional interesting result of these calculations is the identification of a new quasicollective excitation in small metal particles that has, to our knowledge, gone largely unnoticed until now. In the case of the simple metals, the analogy between the scattering processes at a flat surface and at the surface of a spherical particle suggests that the local-field enhancement caused by the dipolar surface plasmon[5] at the flat surface gives rise to a corresponding collective electronic excitation in simple metal particles. A spectral feature in the relevant frequency range above the Mie resonance has indeed been found by Ekardt[16] in his microscopic calculations of the particle polarizability. Recent absorption spectra on relatively large K clusters (500 and 900 atoms) also exhibit a weak structure at this frequency.[12] We believe that this mode represents an excitation that has dipolar angular character but with an additional node in the radial distribution of the dynamical surface screening charge compared to that of the principal Mie plasma oscillation. In the case of Ag particles, this mode cannot be resolved because of the close proximity of the Mie resonance to the volume-type collective excitation.

In a recent paper, Tarriba and Mochán[17] presented a model for the dynamical response of Ag surfaces which is based on a lattice of polarizable dipoles embedded in a homogeneous electron gas with cavities at the sites of the lattice. This model can be viewed as complementary to ours in the sense that it includes the crystalline structure while it neglects the detailed nonlocal response properties of the s electron distribution near the surface. In an alternative approach, Feibelman[18] suggested that the centroid of the induced surface charge at $q=0$ might be shifted inward due to band-structure effects in the surface region. The importance of the polarizable background for the surface plasmon dispersion of Ag was emphasized by Lipparini and Pederiva[19] who used sum-rule arguments to estimate the linear coefficient. Several years ago, in their work on the surface corrections to the Van der Waals reference plane of the noble metals, Zaremba and co-workers[20] represented the centroid of the induced density by a superposition of s and d contributions which were taken from independent calculations for the jellium model and dielectric solid, respectively. For the optical

case, Apell and Holmberg[21] modified this approach by taking into account the actual macroscopic fields in the bulk. However, in none of these calculations was a sufficiently detailed evaluation of the s electron response performed. As the results discussed below demonstrate, a self-consistent treatment of the combined s-d electron system is crucial for an adequate description of the surface-plasmon dispersion of Ag.

This paper is organized as follows. In Sec. II we briefly review the calculation of the excitation spectra of flat simple metal surfaces. It is shown that, in the limit of small q, the exact surface response function can be expressed in terms of an effective local dielectric function involving a complex self-energy. Section III constitutes the main part of this work, namely, the evaluation of the electronic excitations at flat Ag surfaces for the two-component s-d electron system. In Sec. IV, the complex polarizability of small simple metal particles is discussed in terms of a similar self-energy as for the flat surface. In Sec. V we combine the arguments of the two previous sections in order to obtain an expression for the polarizability of small Ag particles. A summary is given in Sec. VI. A preliminary discussion of the results for the Ag surface plasmons dispersion was presented in Ref. 22 and for the Ag Mie resonance in Ref. 11.

II. SIMPLE METAL SURFACES

Let us first review the excitation spectra of simple metal surfaces in order to introduce various quantities and to illustrate the essential features of the surface-plasmon dispersion. In the absence of retardation effects, the probability of exciting electron-hole pairs or collective modes at a flat simple metal surface via inelastic scattering of electrons can be calculated from the imaginary part of the surface response function which may be expressed as[23] (atomic units are used throughout unless stated otherwise):

$$g(q,\omega)=\int dz\, e^{qz}\delta n(z,q,\omega)\ , \tag{2.1}$$

where $q=|\mathbf{q}_{\parallel}|$ is the absolute value of the parallel component of the transferred momentum and $\delta n(z,q,\omega)$ is the surface charge density induced by an external potential of the form $\phi_{\rm ext}(\mathbf{r},t)=-(2\pi/q)\exp(qz+i[\mathbf{q}_{\parallel}\cdot\mathbf{r}_{\parallel}-\omega t])$. We adopt the jellium model whose positive charge background is assumed to occupy the half-space $z\le 0$. Within the TDLDA,[15] the induced density is derived from the expression

$$\delta n(z,q,\omega)=\int dz'\chi(z,z',q,\omega)\phi_{\rm scf}(z',q,\omega) \tag{2.2}$$

with

$$\phi_{\rm scf}=\phi_{\rm ext}+\delta\phi+\delta V_{\rm xc} \tag{2.3}$$

and $\phi_{\rm ext}(z)=-(2\pi/q)\exp(qz)$. The independent-particle response function χ is calculated within the local-density approximation (LDA) for a semi-infinite electron gas with a volume density given by $\bar{n}=3/(4\pi r_s^3)$. The Poisson equation for the induced potential reads as

$$\delta\phi''(z,q,\omega)-q^2\delta\phi(z,q,\omega)=-4\pi\delta n(z,q,\omega) \tag{2.4}$$

and the exchange-correlation term is given by

$$\delta V_{\rm xc}(z,q,\omega)=[\partial V_{\rm xc}(n)/\partial n]|_{n=n_0(z)}\delta n(z,q,\omega)\ , \tag{2.5}$$

where $V_{\rm xc}$ is the local ground-state exchange-correlation potential. In a random-phase approximation (RPA) treatment of the dynamical response this term is omitted from the self-consistent potential $\phi_{\rm scf}$.

Figure 1(a) shows the frequency dependence of the surface loss function, $\mathrm{Im}g(q,\omega)$, for K ($r_s=5$) at several wave vectors q. The volume plasma frequency of this system in the jellium model is $\omega_p=\sqrt{4\pi\bar{n}}=4.2$ eV. The main peak near $\omega_s=\omega_p/\sqrt{2}=3.0$ eV corresponds to the usual monopole surface plasmon whose frequency $\omega_s(q)$ first shifts downwards at small q and subsequently increases for q larger than about 0.15 Å^{-1}. The width of this peak is caused by coupling of the surface plasmon to the excitation of electron-hole pairs. The weaker spectral feature above $\omega_m\approx 0.8\omega_p=3.4$ eV corresponds to the so-called "dipolar" surface plasmon whose charge fluctuation normal to the surface has an extra node compared to the "monopole" charge distribution associated with the ordinary surface plasmon.[5] In Sec. IV we will show that an analogous "multipole" excitation in addition to the standard Mie resonance exists also in the absorption spectrum of simple metal particles.

The calculated momentum dispersion of both monopole and dipole surface plasmons for K is compared in Fig. 1(b) with the experimental results obtained from electron-energy-loss spectra.[5] Since the theoretical results do not include the influence of core polarization, the frequencies of these modes have been scaled down by a factor 0.92 in order to make them coincide with the measured surface-plasma frequency at $q=0$. The LDA results for the monopole and dipole surface plasmons lie at slightly lower frequencies than those obtained within the RPA since the exchange-correlation term makes the induced potential slightly more attractive than the bare Coulomb contribution. The overall agreement between the calculated and measured dispersions is seen to be remarkably good. Similar agreement is found for other simple metals (Al, Na, Cs).[5] In all cases, the monopole surface plasmon at small q seems to be somewhat better described by the RPA response treatment while at larger q the data agree better with the results obtained within the TDLDA. This trend is presumably related to the nature of the local-density approximation which becomes more appropriate for short-wavelength perturbations. The data for the dipole plasmon of K are much better represented by the TDLDA results than by those obtained within the RPA. For other simple metals, on the other hand, the experimental uncertainties are larger, so that a unique identification with either response calculation is less feasible.

The initial negative slope of the monopole surface plasmon that is found for all simple metals, is closely related to the position of the surface screening charge relative to the edge of the jellium background.[6] This may be seen by expanding the surface loss function at small q:[7]

$$g(q,\omega)=\frac{\epsilon(\omega)-1+qd(\omega)[\epsilon(\omega)-1]}{\epsilon(\omega)+1-qd(\omega)[\epsilon(\omega)-1]}\ , \tag{2.6}$$

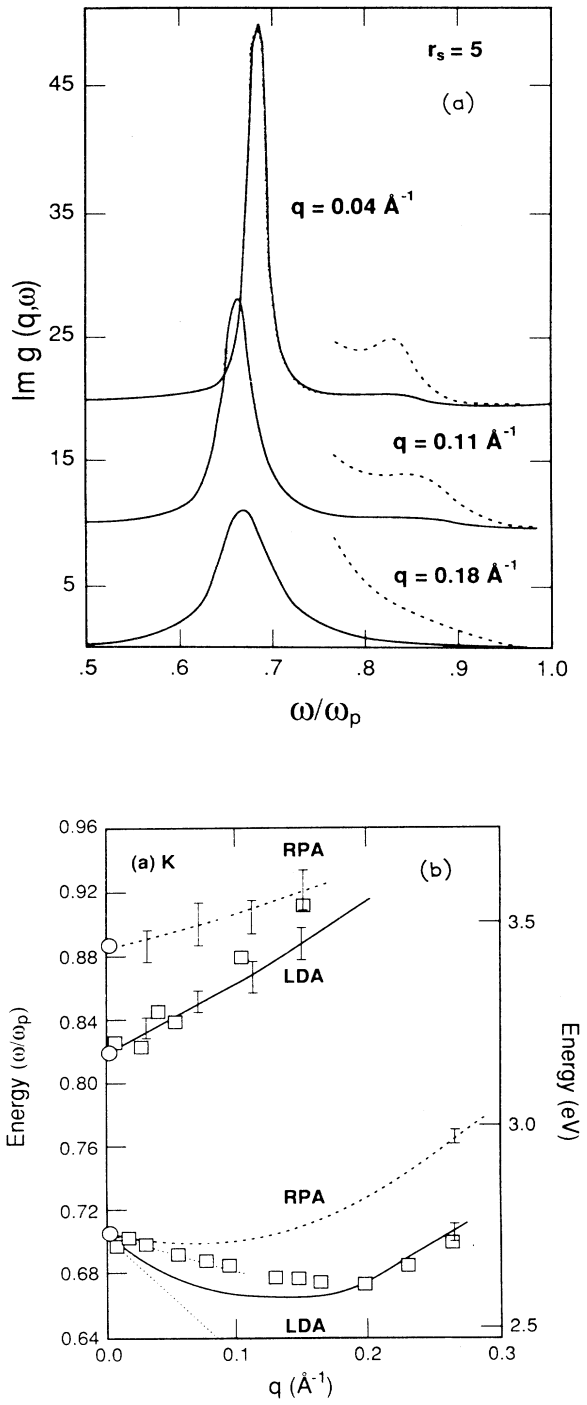

FIG. 1. (a) Frequency dependence of the surface loss function $\mathrm{Im}g(q,\omega)$ (in a.u.), Eq. (2.1), for K at several wave vectors q. The main peak corresponds to the ordinary monopole surface plasmon, the weaker feature above ω_m to the dipolar surface plasmon. (b) Dispersion of monopole and multipole surface plasmons for K. The squares denote the experimental results, the solid curves represent the theoretical surface modes obtained within both the TDLDA and RPA. The vertical bars indicate the uncertainties of the calculated frequencies (Ref. 5).

where $\epsilon(\omega)=1-\omega_p^2/\omega^2$ is the Drude dielectric function, and $d(\omega)$ is the centroid of the surface screening charge induced by an electric field normal to the surface, measured from the edge of the positive charge background

$$d(\omega)=\int dz\, z\delta n(z,0,\omega)\Big/\int dz\,\delta n(z,0,\omega)\ . \tag{2.7}$$

The second surface response function $d_\parallel(\omega)$ for electric fields parallel to the surface vanishes in this geometry.[7] From the pole of the surface response function we find that the dispersion relation of the surface plasmon at small q is given by[6,7]

$$\omega_s(q)=\omega_s[1-\tfrac{1}{2}q\,\mathrm{Re}d(\omega_s)+O(q^2)]\ . \tag{2.8}$$

Since $\mathrm{Re}d(\omega_s)$ is positive for all simple metals,[7,24,25] the surface scattering processes cause a linear redshift at small q. Such a shift is to be expected since with increasing q the induced potential samples a region of lower average density.[4]

For the purpose of the discussion in the following sections, we now introduce an effective local dielectric function $\epsilon(q,\omega)$ as

$$\epsilon(q,\omega)=1-\frac{\omega_p^2}{\omega^2+\Sigma(q,\omega)}\ , \tag{2.9}$$

where the self-energy is given by

$$\Sigma(q,\omega)=qd(\omega)(\omega_p^2-\omega^2)\ . \tag{2.10}$$

With these definitions the surface response function acquires the simple form

$$g(q,\omega)=\frac{\epsilon(q,\omega)-1}{\epsilon(q,\omega)+1}=\frac{\omega_s^2}{\omega_s^2-\omega^2-\Sigma(q,\omega)}\ . \tag{2.11}$$

Note that this expression is exact to lowest order in q. Thus the true nonlocal surface response at small q has been reformulated in terms of a "classical" dielectric function whose self-energy accounts for the quantum-mechanical surface effects and the nonlocal aspects of the response. Equation (2.11) shows that the effects described by the complex self-energy lead to the damping of the surface plasmon and to the shift of its frequency from the classical value.

For completeness we point out that $\mathrm{Im}d(\omega)$, and accordingly also $\mathrm{Im}\Sigma(q,\omega)$, can be expressed in terms of the golden rule formula[26,27]

$$\mathrm{Im}\Sigma(q,\omega)=q(\omega_s^2-\omega^2)\frac{1}{\pi^3}$$
$$\times\Sigma'\int_0^{k_F}dk\frac{h(k)}{k'}|\langle k'|\phi_{\mathrm{scf}}|k\rangle|^2\ , \tag{2.12}$$

where $k'=\sqrt{k^2+2\omega}$ and $h(k)=\min[2\omega,k_F^2-k^2]$. Here, k_F is the Fermi wave vector and ϕ_{scf} is the long-wavelength limit of the self-consistent potential appearing in the response equation (2.2). (The frequency-dependent prefactor cancels a corresponding inverse frequency variation of ϕ_{scf}.) The primed sum denotes the summation over possible final-state channels. This formula allows a convenient identification of the electronic transitions that contribute to the total absorption cross

section, in particular, those that correspond to "internal" excitation (the excited electron propagates towards the interior of the bulk) and, above threshold, to emission into the vacuum.

Figure 2(a) shows the frequency dependence of the self-energy $\Sigma(q,\omega)$ for a volume density corresponding to Na (density parameter $r_s=4$). These results are obtained from TDLDA calculations of the centroid function $d(\omega)$.[24] $\mathrm{Re}\Sigma(q,\omega)$ is seen to be positive approximately up to the multipole surface plasma frequency $\omega_m=0.8\omega_p=4.7$ eV. This is a consequence of the fact that the centroid of the surface screening charge is located in the tail of the ground-state electron density, i.e., outside of the edge of the positive background. According to Eq. (2.10), the low-frequency limit of $\mathrm{Re}\Sigma(q,\omega)$ is, in fact, just determined by the position of the static image plane $d(0)$. Beyond the multipole frequency, screening at the surface becomes less efficient and the charge centroid shifts towards the interior of the metal. As ω approaches the threshold of transparency $\omega_p=5.9$ eV, $\mathrm{Re}d(\omega)$ diverges towards $-\infty$.[7,24,25] The self-energy, on the other hand, vanishes at this frequency since the external electron cannot excite a volume plasmon of infinite wavelength. $\mathrm{Im}\Sigma(q,\omega)$ shows a strong enhancement near ω_m.[7,24,25] Similar features at nearly the same relative frequency are found for other jellium systems with different volume densities. The strength of this mode, however, depends sensitively on the value of r_s. For the low-density alkali metals with their more diffuse density profile at the surface, the multipole plasmon is much stronger and more narrow than in the case of Al.

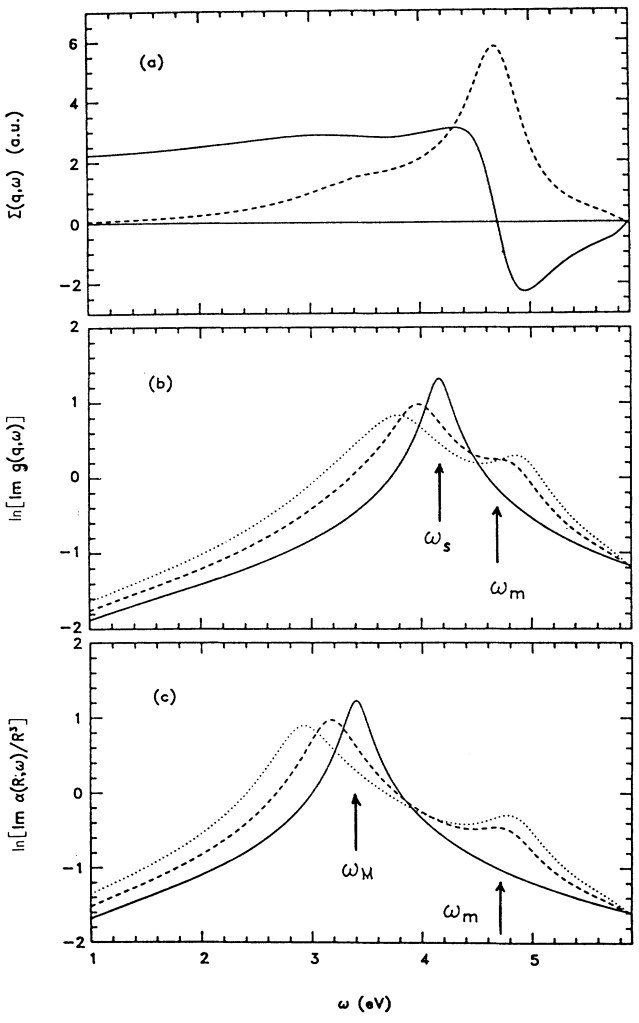

FIG. 2. (a) Frequency dependence of the self-energy $\Sigma(q,\omega)$, Eq. (2.9), for the semi-infinite electron gas with bulk electronic density corresponding to Na ($r_s=4$) and $q=0.05$ a.u. Solid curve: real part, dashed curve: imaginary part. (b) Logarithm of the surface loss function $\mathrm{Im}g(q,\omega)$, Eq. (2.11), for Na at $q=0$ (solid curve), $q=0.025$ a.u. (dashed curve), and $q=0.05$ a.u. (dotted curve). (c) Logarithm of normalized particle polarizability $\mathrm{Im}\alpha(R,\omega)/R^3$, Eq. (4.3), for Na at $R\to\infty$ (solid curve), $R=40$ a.u. (dashed curve), and $R=20$ a.u. (dotted curve).

In Fig. 2(b) the surface loss function $\mathrm{Im}g(q,\omega)$ calculated from Eq. (2.11) is shown for several values of q. [In the loss function for $q=0$, a damping parameter $\gamma=0.2$ eV is included in the Drude function $\epsilon(\omega)$.] The main loss feature near $\omega_s=\omega_p/\sqrt{2}=4.2$ eV corresponds to the excitation of the surface plasmon which is redshifted and broadened as a result of the self-energy processes. The smaller peak above $\omega_m=0.8\omega_p=4.7$ eV corresponds to the excitation of the multipole surface plasmon. In contrast to the monopole surface plasmon, it exhibits a positive dispersion at small q. The comparison of these results with exact loss function demonstrates that the self-energy formulation at small q yields an accurate representation of the physical mechanisms that are responsible for the shift and broadening of the collective surface excitations.

We finally point out that, as can be seen in Fig. 2(a), $\Sigma(q,\omega)$ exhibits a weak second spectral feature close to the threshold for emission, i.e., near $\omega\approx\Phi$ where $\Phi=3.1$ eV is the work function.[24] In the present case, this feature is dominated by the main dipolar surface-plasmon peak. For higher bulk densities[24] or for submonolayer alkali-metal overlayers,[28] on the other hand, this threshold excitation mechanism can become quite prominent. The increased loss probability in this range is not caused by the larger one-electron density of states close to the top of the surface barrier. Instead, it was recently shown to be a consequence of surface screening processes and of matrix element effects.[29]

III. Ag SURFACES

In this section we extend the response formalism described above in order to include the main influence of the filled $4d$ bands on the surface-plasmon dispersion relation of Ag. As discussed in the Introduction, we focus on the modification of the intraband transitions due to the mutual s-d polarization since the frequency of the Ag surface collective excitations lies below the region of interband transitions. Thus, we assume that the $5s$ electrons can be characterized by the nonlocal surface response function $\chi(z,z',q,\omega)$ of a semi-infinite jellium system. The neutralizing positive background is located in the half-space $z\leq 0$. The influence of the $4d$ electrons

is represented via the same local dielectric function $\epsilon_d(\omega)$ as in the bulk; the position of the boundary up to which this polarizable medium is assumed to extend is denoted by z_d. This distance which is the only free parameter in our model, should be located somewhere between the edge of the positive background and the first plane of nuclei. Figure 3(a) shows in a schematic way the model on which our calculations are based. The frequency dependence of the real and imaginary parts of the bound term $\epsilon_d(\omega)$ and of the real part of the measured dielectric function $\epsilon(\omega)$ are shown in Fig. 3(b).

The electronic surface excitations of Ag will be calculated from the surface response function $g(q,\omega)$ as defined in Eq. (2.1). The Poisson equation for the induced potential, however, now reads as

$$\delta\phi''(z,q,\omega)-q^2\delta\phi(z,q,\omega)=-4\pi\delta n(z,q,\omega)/\epsilon_d(z,\omega) , \tag{3.1}$$

where $\epsilon_d(z,\omega)=\epsilon_d(\omega)\Theta(z_d-z)$. At the boundary of the polarizable medium representing the d states, the total electrostatic potential $\phi=\phi_{\rm ext}+\delta\phi$ satisfies the boundary condition ($z_d^{\pm}=z_d\pm\delta$)

$$\epsilon_d(\omega)\phi'(z_d^-,q,\omega)=\phi'(z_d^+,q,\omega) . \tag{3.2}$$

In order to solve the response equation for the model outlined above we write the Coulomb part of the self-consistent potential as

$$\phi=\phi_{\rm ext}+\phi_1+\phi_2 \tag{3.3}$$

where $\phi_{\rm ext}(z)=-(2\pi/q)\exp(qz)$ and

$$\phi_1(z,q,\omega)=\frac{2\pi}{q}\int dz' e^{-q|z-z'|}\delta n(z',q,\omega)/\epsilon_d(z',\omega) , \tag{3.4}$$

$$\phi_2(z,q,\omega)=\frac{2\pi}{q}ae^{-q|z-z_d|} . \tag{3.5}$$

This latter term is introduced to ensure the discontinuity of the Coulomb potential specified in Eq. (3.2). The coefficient a is determined as follows. Let us define

$$\phi_1'(z_d,q,\omega)=-2\pi b \tag{3.6}$$

with

$$b=\int dz' e^{-q|z_d-z'|}\mathrm{sgn}(z_d-z')\delta n(z',q,\omega)/\epsilon_d(z',\omega) . \tag{3.7}$$

From Eq. (3.5) we have

$$\pm\phi_2'(z_d^{\pm},q,\omega)=-2\pi a . \tag{3.8}$$

Thus,

$$\phi'(z_d^{\pm},q,\omega)=-2\pi(A\pm a) \tag{3.9}$$

with

$$A=e^{qz_d}+b . \tag{3.10}$$

The condition (3.2) then implies

$$\epsilon_d(\omega)(A-a)=A+a \tag{3.11}$$

or

$$a=A\frac{\epsilon_d(\omega)-1}{\epsilon_d(\omega)+1}\equiv A\sigma_d(\omega) . \tag{3.12}$$

The final expression for the Coulomb potential therefore reads as

$$\phi(z,q,\omega)=\bar{\phi}_{\rm ext}(z,q,\omega)+\delta\bar{\phi}(z,q,\omega) , \tag{3.13}$$

where

$$\bar{\phi}_{\rm ext}(z,q,\omega)=-\frac{2\pi}{q}e^{qz}+\frac{2\pi}{q}\sigma_d(\omega)e^{-q|z-z_d|}e^{qz_d} \tag{3.14}$$

and

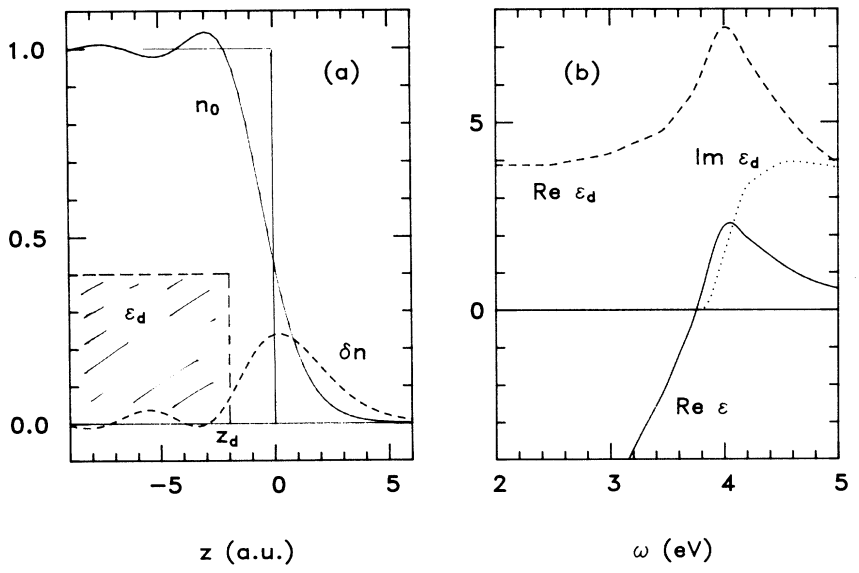

FIG. 3. (a) Schematic model for dynamical response of two-component 5s-4d electron system. Solid curve: ground-state density profile of 5s electrons; dashed curve: induced density. The positive background is located in the half-space $z\leq 0$; the polarizable medium representing the 4d states extends up to $z\leq z_d$. (b) Frequency dependence of real and imaginary parts of the "bound" dielectric function $\epsilon_d(\omega)$ (dashed and dotted curves, respectively). Solid curve: real part of measured dielectric function of bulk Ag (Ref. 30).

$$\delta\bar{\phi}(z,q,\omega)=\frac{2\pi}{q}\int dz'\delta n(z',q,\omega)/\epsilon_d(z',\omega)[e^{-q|z-z'|}+\sigma_d(\omega)e^{-q|z-z_d|}e^{-q|z'-z_d|}\mathrm{sgn}(z_d-z')] . \quad (3.15)$$

The presence of the polarizable medium representing the $4d$ states is seen to cause a renormalization of the external potential and of the Coulomb response kernel. Apart from these modifications the structure of the response equation is the same as that for the simple metals discussed in the previous section. We have solved these new response equations self-consistently without further approximations. Since we are here concerned only with the surface-plasmon dispersion, propagating bulk-plasmon modes do not need to be taken into account.

Figure 4 shows several calculated surface excitation spectra at different values of q. The boundary of the polarizable medium is in this case located at $z_d=0$. The main peak in these spectra corresponds to the surface plasmon which is seen to shift to higher frequencies with increasing q. The spectra weight above 3.8 eV corresponds to transitions from the d band as illustrated in Fig. 3(b). We have found no evidence for the existence of a multipole surface-plasmon mode. The frequency range between the ordinary surface plasmon and the interband transitions is presumably too narrow to sustain this higher-order collective surface excitation.

Typical surface densities induced by the external potential are shown in Fig. 5. At low frequencies, the density is localized within a few Å of the surface with only the weak Friedel oscillations decaying more slowly towards the interior. Near the surface-plasma frequency, on the other hand, the induced density is seen to extend much farther into the bulk because of the close proximity to the transparency threshold of Ag. This behavior differs from that on the simple metals where the density fluctuation of the surface plasmon remains rather concentrated near the surface because of the larger frequency separation from the volume plasmon.[24]

The dispersion of the Ag surface plasmon for $z_d=0$ is compared in Fig. 6(a) with the corresponding dispersion in the absence of the s-d interaction, i.e., for a semi-infinite electron gas with $r_s=3$. In the latter case, the surface plasmon exhibits the behavior that is typical for

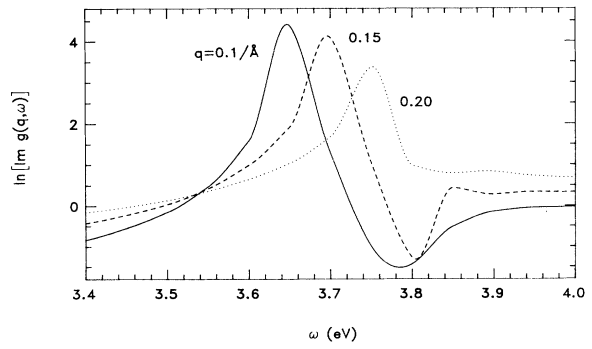

FIG. 4. Frequency dependence of logarithm of surface loss function $\mathrm{Im}g(q,\omega)$ for Ag at several wave vectors q for $z_d=0$ (TDLDA).

all simple metals,[5] with a negative initial slope given by $d(\omega)$, the centroid of the screening charge in the $q=0$ limit.[4–7] The LDA response leads to slightly lower frequencies than the RPA because the more attractive induced potential in the surface region pulls the surface charge somewhat farther into the vacuum. The s-d interaction is seen to cause not only an overall lowering of the plasma frequency by about 3 eV but also a strong upward distortion of the dispersion with q: In the RPA, the negative slope at small q has disappeared so that the plasma frequency now rises monotonically with q. Only in the LDA treatment is there a remnant of a weak minimum at very small q.

The variation of the surface-plasmon dispersion with the parameter z_d is shown in Fig. 6(b). For the sake of clarity, only the RPA curves are plotted; the LDA results lie slightly lower. In the limit of small q, these curves converge, as they should, to the frequency ω_s^* which is determined solely by the bulk dielectric function and therefore must be independent of z_d. At finite q, the dispersion is seen to be positive for $z_d\leq 0$. Thus, the absence of the s-d interaction in the vacuum region causes a blueshift of the surface-plasma frequency with increasing q. This effect becomes more pronounced as z_d is shifted deeper inside since the unscreened portion of the plasma oscillation is enhanced. Conversely, if the boundary z_d is located outside the surface, the induced surface density is more fully screened at all q, so that the dispersion shows an initial negative slope just as on the simple metal surfaces.

In the jellium model, the edge of the positive background is located half a lattice spacing above the first plane of nuclei. In the case of the Ag (111), (001), and (110) faces, this distance d_0 amounts to 1.18, 1.02, and 0.72 Å, respectively. The theoretical results in Fig. 6(b) show that, for z_d in the range $-d_0\leq z_d\leq 0$, the surface-plasmon dispersion within our model is positive and that the overall slope agrees qualitatively with the data. For the Ag (001) and (111) crystal faces these are indicated by the dotted and dashed lines, respectively.[1–3] These curves have been rigidly shifted downwards by 0.06 eV in order to make them coincide with $\omega_s^*(q=0)$ obtained from the measured bulk dielectric function.[30] For the (110) face the dispersion along the rows is similar to that on Ag (111) whereas across the rows, the dispersion is nearly the same as on Ag (001).[3] For completeness, the measured dispersion of the Ag bulk plasmon[31] is also shown in Fig. 6(b). Obviously, the dependency of the dispersion on the crystal face and the anisotropy on the (110) face are beyond the scope of the present model since it is based on a homogeneous polarizable medium that is abruptly terminated at a fixed distance from the surface. Crystallinity could be approximately incorporated, for example, by treating the $4d$ states as polarizable shells located at the sites of an fcc lattice. It is possible, however, that band-structure effects must also be taken into account in order to understand the more detailed aspects of

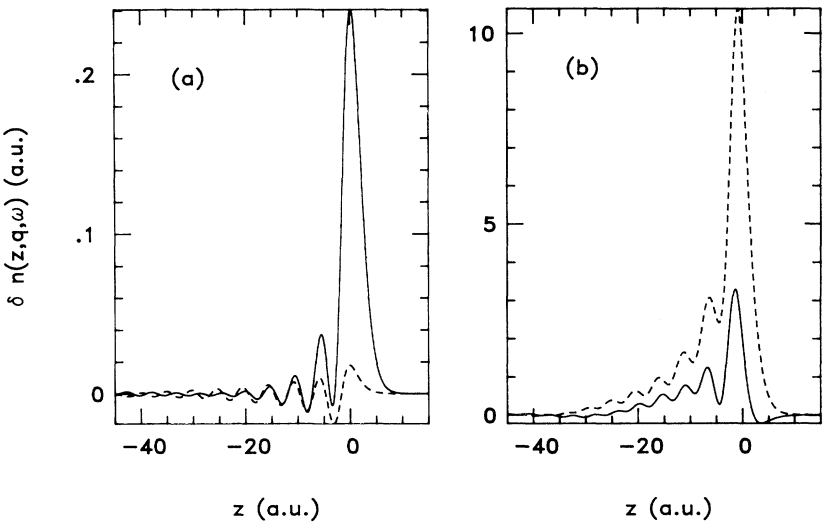

FIG. 5. Induced density $\delta n(z,q,\omega)$ for $q=0.15$ Å^{-1} (TDLDA). (a) $\omega=1.0$ eV; (b) $\omega=3.7$ eV. Solid curves: real part; dashed curves: imaginary part.

the observed dispersions.

The dispersions shown in Fig. 6 are the main result of this work. It is clear that even in the low-frequency range where essentially only intraband transitions within the nearly free-electron s-p band of Ag contribute, the polarization influence of the lower-lying filled $4d$ band has a very strong effect on the surface-plasmon dispersion. An alternative way of interpreting these results is the following: The large redshift from the bare plasmon frequency $\omega_s(q)$ to the screened one, $\omega_s^*(q)$, due to the mutual polarization of s and d states, depends strongly on q: It is largest in the limit of small q because the induced field decays very slowly into the solid (see illustration in Fig. 7). With increasing q, this field decays more rapidly and the s-d interaction is gradually "switched off." This q-dependent reduction of the mutual s-d polarization leads to an upward skewing of the surface-plasmon dispersion.

For the purpose of the discussion in Sec. V on the Ag particles, we conclude this section by giving a reformulation of the above results at small q in terms of a complex self-energy. In analogy to Eq. (2.11), we write the Ag surface loss function at small q in the form

$$g(q,\omega)=\frac{\epsilon(q,\omega)-1}{\epsilon(q,\omega)+1}\ , \tag{3.16}$$

where the effective dielectric function is now given by

$$\epsilon(q,\omega)=1-\frac{\omega_p^2}{\omega^2+\Sigma(q,\omega)}+\Delta(\omega) \tag{3.17}$$

with $\Delta(\omega)=\epsilon_d(\omega)-1$. At frequencies close to the surface plasmon the self-energy can be parametrized as

$$\Sigma(q,\omega)=qD(\omega)\omega_s^{*2}\ , \tag{3.18}$$

where $\omega_s^*\approx\omega_p/\sqrt{2+\mathrm{Re}\Delta}\approx 3.64$ eV. Thus, as in Eq. (2.11), the exact nonlocal surface response at small q is rewritten in terms of a "classical" dielectric function whose self-energy accounts for the quantum-mechanical surface effects and the nonlocal aspects of the response. According to the poles of $g(q,\omega)$, the dispersion of the Ag surface plasmon at small q is given by

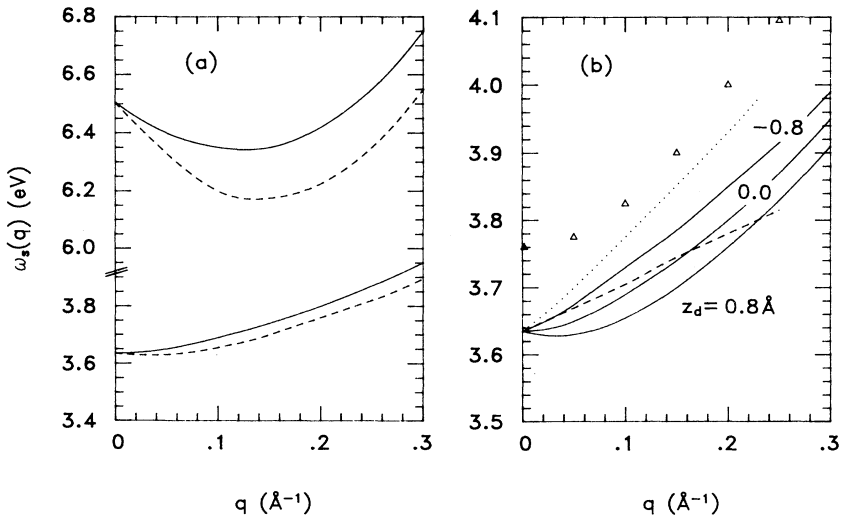

FIG. 6. (a) Dispersion of surface plasmon of Ag for $z_d=0$ (lower curves) and of semi-infinite electron gas with $r_s=3$ (upper curves). Solid lines: RPA response treatment; dashed lines: TDLDA. (b) Dispersion of surface plasmon of Ag for $z_d=0$ and $z_d=\pm 0.8$ Å calculated within RPA (solid curves). The dotted and dashed lines denote the measured dispersions for the (001) and (111) faces of Ag, respectively (see text) (Refs. 1 and 3). The triangles indicate the measured dispersion of the volume plasmon (Ref. 31).

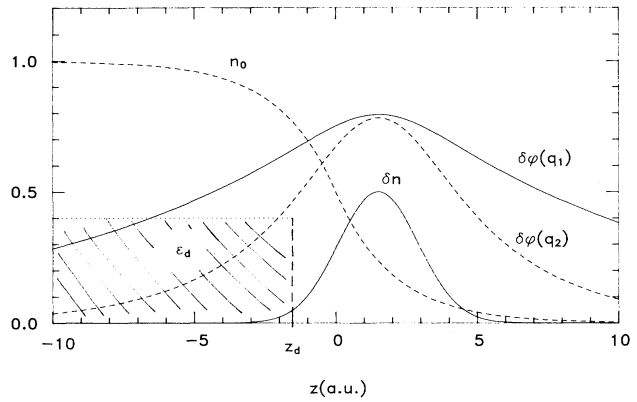

FIG. 7. Schematic illustration of induced density $\delta n(z,q,\omega)$ associated with Ag surface plasmon and corresponding electrostatic potential $\delta\phi(z,q,\omega)$. With increasing $q_2 > q_1$, the range of this potential decreases and its overlap with the polarizable medium ϵ_d representing the $4d$ states is reduced. Thus, the s-d screening interaction is gradually "switched off."

$$\omega_s^*(q) \approx \omega_s^*[1-0.5qD_s+O(q^2)] , \tag{3.19}$$

where $D_s = \mathrm{Re}D(\omega_s^*)$. The experimental curves[1-3] in Fig. 6(b) for the (111) and (001) faces correspond to $D_s \approx -0.4$ and -0.8 Å, respectively. The two orthogonal directions on the Ag(110) face yield nearly the same coefficients. As we have shown above, our calculations give slopes of similar magnitude if the boundary of the polarizable medium representing the d states is located between the first plane of Ag nuclei and the edge of the background that neutralizes the s electrons. In Sec. V we will use this approximate representation of the surface loss function to estimate the complex polarizability of Ag particles.

IV. SIMPLE METAL PARTICLES

We now show that the electronic excitations at simple metal surfaces discussed in Sec. II have a close relationship to those observed in optical-absorption spectra of small simple metal particles. A similar correspondence was derived earlier by Apell and Ljungbert[32] using a rather different approach. The particle radii we are considering here extend up to about 100 Å, i.e., $R \ll c/\omega$ so that retardation effects are negligible. Moreover, we only discuss here the interaction of the particles with light, i.e., only the excitation of the dipole mode is of interest. The complex dipole polarizability of small jelliumlike metal particles may be calculated by using the time-dependent density-functional approach.[15] In analogy to the response function of the flat surface, we write this polarizability as

$$\alpha(R,\omega) = R^3 \frac{\epsilon(R,\omega)-1}{\epsilon(R,\omega)+2} , \tag{4.1}$$

where R is the radius of the positive background. The effective local dielectric function $\epsilon(R,\omega)$ is given by

$$\epsilon(R,\omega) = 1 - \frac{\omega_p^2}{\omega^2+\Sigma(R,\omega)} . \tag{4.2}$$

The complex self-energy $\Sigma(R,\omega)$ accounts for scattering processes and nonlocal effects at the surface of the particle. Using this definition the particle polarizability takes the form

$$\alpha(R,\omega) = R^3 \frac{\omega_M^2}{\omega_M^2-\omega^2-\Sigma(R,\omega)} \tag{4.3}$$

with $\omega_M = \omega_p/\sqrt{3}$. Thus $\Sigma(R,\omega)$ determines the shift and broadening of the classical Mie resonance.

Since we are here concerned with a qualitative discussion of the absorption spectra of small metal particles, we will not attempt to calculate the self-energy from first principles. Instead we now make the assumption that, in the limit of large R, the response properties at the surface of a spherical particle should become similar to those at a flat metal surface in the long-wavelength limit. This assumption seems justified since the quantum-mechanical scattering processes contributing to the self-energy occur within a very narrow region in the vicinity of the surface. In analogy to the definition (2.10) we therefore approximate $\Sigma(R,\omega)$ as

$$\Sigma(R,\omega) \approx R^{-1} d(\omega)(\omega_p^2-\omega^2) , \tag{4.4}$$

where $d(\omega)$ should have a similar magnitude and spectral dependence as the corresponding centroid for the flat surface. Inserting Eq. (4.4) into (4.3), it is easily verified that the above choice of $\Sigma(R,\omega)$ is consistent with the static limit of the particle polarizability which is given by

$$\alpha(R,0) = [R+d(0)]^3 . \tag{4.5}$$

This expression indicates the well-known fact that the effective radius of the particle is larger than R since the centroid of the polarization charge is located outside the edge of the positive background.[33] An explicit $1/R$ dependence of a slightly different self-energy was derived earlier by Zaremba and Persson[34] in their approximate self-consistent scheme for the evaluation of the particle polarizability. Since the variable $1/R$ is a measure of the surface-to-volume ratio, it plays the same role as q in the case of the flat surface. Thus, the results shown in Fig. 2(a) for the self-energy of the flat surface can be taken as representative of the corresponding self-energy for spherical metal particles.

From Eqs. (4.3) and (4.4) we obtain the following expression for the size dependence of the Mie resonance at large R:

$$\omega_M(R) = \omega_M[1-R^{-1}\mathrm{Re}d(\omega_M)+O(R^{-2})] . \tag{4.6}$$

Since $\mathrm{Re}d(\omega_M) > 0$ for simple metals, the surface scattering processes cause a linear redshift with decreasing radius and the linear coefficient is given by the centroid of the dynamical screening charge in the large R limit. This size dependence of the Mie resonance agrees with the one found by Apell and Ljungbert.[32]

Figure 2(c) shows the frequency dependence of the imaginary part of the polarizability of a Na particle in the limit $R \to \infty$ and for two finite radii, calculated from Eq. (4.1). The main spectral feature near $\omega_M = 3.4$ eV corresponds to the Mie resonance which is redshifted and

broadened due to the self-energy processes at the surface of the particle. The comparison with the results shown in Fig. 2(b) suggests that the other peak above the Mie resonance is caused by a similar local-field enhancement as the multipole surface plasmon on the flat surface. This mode exhibits a blueshift with decreasing particle size.

A comparison of our results for the frequency dependence of $\mathrm{Im}\alpha(R,\omega)/R^3$ with the exact calculations of Ekardt[16] and with the self-energy calculations of Zaremba and Persson[34] is shown in Fig. 8 for a Na particle of radius $R=23.3$ a.u. Apart from the fine structure caused by interlevel transitions which is, of course, absent in the self-energy approaches, there is remarkable overall agreement between these different calculations. In particular, the close resemblance of our results to the full quantum-mechanical calculations indicates that the ansatz for the particle self-energy in (4.4) is reasonable. Nevertheless, our results differ in some important aspects from those in Ref. 34. While the redshift of the Mie plasmon from 3.4 to about 3.0 eV obtained in the present work agrees well with the one found by Ekardt, the results in Ref. 34 show a curious double peak structure. This arises from a very large self-energy effect close to the ionization threshold which in this particular example happens to lie at about $\Phi=3.1$ eV, i.e., just below the Mie resonance. As discussed above, our results also exhibit a feature near this threshold but it is very much weaker than the one found in Ref. 34. Similar discrepancies exist at other bulk densities (compare Fig. 7 in Ref. 34 and Fig. 2 of Ref. 24).

It is evident from Fig. 8 that the detailed calculations in Ref. 16 show a spectral feature between the main Mie resonance and the volume plasma frequency. It seems plausible that this peak has the same physical origin as the multipole surface plasmon at ω_m on the flat surface. The nature of this excitation could be investigated in more detail by determining the position of the dynamical charge centroid in jellium particles. If an inward shift is found as the frequency increases from the Mie resonance to the volume plasma frequency, this would be convincing evidence for the similarity of the particle surface scattering processes and those at the flat metal surface. Such a resonance-type behavior of the centroid of the induced density in the vicinity of ω_m seems to have indeed been found in microscopic calculations of the particle polarizability.[35] As shown in Fig. 8 this feature should disperse towards higher frequencies with decreasing particle radius. Moreover, the relative intensity of this mode should be considerably stronger for metals with lower average density (see Fig. 2 in Ref. 24). In the approach by Zaremba and Persson[34] neither the self-energy or the particle polarizability show any structure in the vicinity of this multipole surface-plasma resonance. Presumably this peak is absent in their approach because of the additional approximations made in the evaluation of the electrostatic potential entering the expression for the self-energy.

Recent measurements of the absorption cross section of large K particles (500 and 900 atoms) (Ref. 12) do indeed show spectral weight at 2.9 eV, i.e., exactly where we would expect this new collective particle resonance to occur. We suggest performing additional measurements

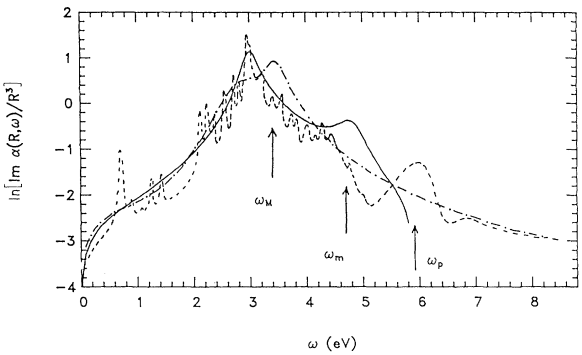

FIG. 8. Frequency dependence of logarithm of normalized polarizability for Na particle of radius $R=23.3$ a.u. Solid curve: present self-energy approach, Eq. (4.3); dashed curve: microscopic results of Ekardt (Ref. 16); dot-dashed curve: self-energy approach of Zaremba and Persson (Ref. 34). The vertical arrows denote the frequencies of the Mie plasmon at $\omega_M=3.4$ eV and of the "dipolar" particle surface plasmon at $\omega_m=4.7$ eV, both in the limit $R=\infty$, and of the volume plasmon at $\omega_p=5.9$ eV.

on large Na, K, Rb, and Cs clusters for varying diameters in order to separate this mode for the main Mie plasma resonance.

As can be seen in Fig. 8, the microscopic calculations of $\mathrm{Im}\alpha(R,\omega)$ by Ekardt also show a spectral feature close to the bulk-plasma frequency of Na. Since the self-energy of the flat surface vanishes at the transparency threshold, the ansatz made in Eq. (4.4) does not allow for volume-type plasmons in metal particles. Obviously, the analogy between surface scattering processes at a flat surface and a particle surface breaks down in this frequency range. The approach used in Ref. 34 also does not include such volume-type plasmon excitations.

V. Ag PARTICLES

In this section we now combine the ideas discussed in Secs. III and IV in order to investigate the optical-absorption spectra of spherical Ag particles in the limit of large radii. As pointed out in the Introduction, small Ag particles exhibit a blueshift of the Mie resonance peak as a function of decreasing particle radius.[8–11] The earlier measurements were usually taken for Ag clusters embedded in various matrices where the resonance shifts induced by the surrounding medium are actually of the same order or larger than the shifts associated with the finite particle size. The matrix effect can, in fact, be so strong that it leads to a redshift of the resonance.[36] However, the recent experiments on gas-phase Ag particles establish unequivocally the blueshift of the Mie resonance compared to the classical limit.[10,11] This behavior is in striking contrast to the redshift of the Mie resonance of the alkali-metal clusters. As we have discussed in the previous section, this redshift is closely related to the spill-out effect. Thus, just as in the case of the Ag surface-plasmon dispersion, the presence of the filled $4d$ levels changes the sign of the variation of the particle resonance frequency.

The model for combined 5*s*-4*d* response that we have used in Sec. III for the evaluation of the surface-plasmon dispersion could, in principle, also be applied to determine the absorption spectrum of Ag particles. Such a calculation requires the same nonlocal response function for the *s* electrons as in the case of jellium particles. However, the potential associated with the dynamically induced density will now be screened due to the presence of the polarizable medium representing the fully occupied 4*d* states. Since we are only concerned with the limit of large R, this medium can be represented by the same bound dielectric contribution $\epsilon_d(\omega)$ as in the volume. As a result of the *s*-*d* interaction the Mie resonance frequency is reduced from its unscreened value $\omega_M = \omega_p/\sqrt{3} = 5.3$ eV to $\omega_M^* \approx \omega_p/\sqrt{2+\mathrm{Re}\epsilon_d} \approx 3.5$ eV.

The important feature of our model is now, like in the case of a flat Ag surface, that this *s*-*d* interaction is absent in the surface region where the 5*s* electrons spill out into the vacuum. Since part of the density fluctuation associated with the Mie resonance oscillates with the unscreened plasma frequency, this mechanism leads to an increase of the resonance frequency. Moreover, this effect becomes more pronounced with decreasing particle radius because of the larger surface-to-volume ratio. Thus, the Mie resonance frequency exhibits a blueshift with decreasing particle size.

The physical situation is therefore similar to the one illustrated schematically in Fig. 7 with the z axis replaced by the radial coordinate r: Since the radial component of the induced potential is proportional to r in the interior, the overlap with the polarizable medium representing the *d* states is largest for large particle radii [see $\delta\phi(q_1)$ in Fig. 7]. As the particle size is decreased, the induced potential falls off more rapidly [roughly like $\delta\phi(q_2)$] so that this overlap is gradually reduced. Thus, as a function of decreasing radius, the resonance frequency is shifted up towards the unscreened plasma frequency.

Instead of calculating the particle absorption spectrum quantum mechanically within this model, we now employ a similar self-energy approach as in the previous section for the simple metal particles. Thus, we write the effective particle dielectric function as

$$\epsilon(R,\omega) = 1 - \frac{\omega_p^2}{\omega^2 + \Sigma(R,\omega)} + \Delta(\omega) \tag{5.1}$$

with $\Delta(\omega) = \epsilon_d(\omega) - 1$. Furthermore, we assume that the self-energy processes at the surface of a sufficiently large Ag particle are similar to those at a flat Ag surface. Using this approximation we obtain from (3.18)

$$\Sigma(R,\omega) \approx R^{-1} D(\omega) \omega_s^{*2} . \tag{5.2}$$

With this self-energy, the size dependence of the Ag Mie resonance at large R is given by

$$\omega_M^*(R) = \omega_M^* [1 - 0.5 R^{-1} D_M (\omega_s^*/\omega_M^*)^2 + O(R^{-2})] , \tag{5.3}$$

where $\omega_M^* \approx \omega_p/\sqrt{3+\mathrm{Re}\Delta} \approx 3.5$ eV and $D_M = \mathrm{Re}D(\omega_M^*)$. Because of the closeness of the frequencies ω_s^* and ω_M^* this result shows that the linear coefficient for the Mie resonance should be nearly the same as that of the surface plasmon. Figure 9 shows the variation of the Ag Mie resonance with particle radius.[10,11] The solid line corresponds to $D_M \approx -0.85$ Å which agrees quite well with the slope expected from the dispersion of the Ag surface plasmons.

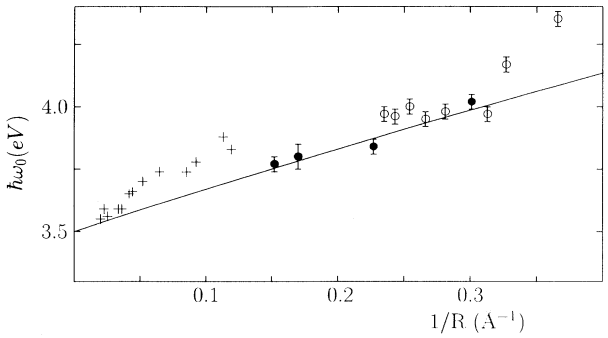

FIG. 9. Variation of Ag Mie resonance with inverse of particle radius. The dots denote experimental data for positively charged gas-phase particles. The + symbols are for Ag particles in an Ar matrix [Ref. 9(a)]. The solid line is a fit through these data and the frequency expected in the limit of large R (Ref. 11).

The above considerations apply to neutral Ag surfaces and particles. For the positively charged clusters studied in Refs. 10 and 11, the effective centroid of the induced *s*-*d* surface density should be located somewhat farther inside the metal, leading to an enhancement of the blueshift. Conversely, the centroids of negatively charged Ag clusters are presumably located outside the surface which should cause a redshift of the Mie resonance with decreasing radius. Such a reversal of the shift upon negative charging has indeed been observed.[37]

We point out that the observed resonance frequencies of small metal particles may be influenced by various other effects. In the present case, slight frequency shifts could, for example, result from the rather high temperature of the sputtered clusters [2000–3000 K (Ref. 38)]. In the bulk, raising the temperature from 300 to about 700 K leads to a redshift of the Ag volume plasma frequency of about 0.1 eV.[39] At higher temperatures, the plasmon loss feature broadens considerably and its main position shifts to higher frequencies. Nevertheless, the resonance frequencies of the small clusters studied here agree quite well with those of Ag clusters in solid Ar at 10 K.[9] Also, the interatomic spacing might not be the same as in the bulk and the concentration of defects might be rather large. These effects, which all produce shifts of the resonance frequency, become particularly severe in very small Ag clusters where the discrete atomic geometry must also be taken into consideration. Transitions between the cluster levels then become important and the description of the absorption spectra in terms of macroscopic quantities becomes inappropriate.

VI. CONCLUSION

The dispersion of the Ag surface plasmon and of the Ag Mie resonance have been discussed in terms of a model for the dynamical response of the 5*s*-4*d* electron sys-

tem. This model makes use of the fact that the frequencies of these collective modes lie below the region of transitions involving the d states. The primary physical effect is therefore the influence of the s-d polarization on the electronic transitions between the low-lying nearly-free-electron s-p states. The nonlocal response properties of these states are treated within the time-dependent density-functional scheme and the d states are represented via a polarizable medium that extends up to a certain distance from the surface. The key feature of this approach is that the s and d electronic densities are considered in a combined, self-consistent manner, i.e., they are not assumed to respond independently of one another to the applied perturbation. Since the s-d interaction is absent in the region where the s electrons spill out into the vacuum, a part of the collective density fluctuation oscillates with the unscreened plasma frequency, leading to a blueshift of the effective s-d surface plasmon.

In the case of the electronic excitations at a flat Ag surface, we obtain the plasmon dispersion within this model from a direct solution of the appropriate response equations in real space. For the Ag particles we use instead a self-energy formulation in conjunction with an effective dielectric function and assume that the scattering processes at the surface of a sufficiently large particle are similar to those occurring at a flat metal surface. This analogy suggests that the linear coefficients of the Ag surface plasmon at small parallel momenta and of the Mie resonance at small inverse radii should be rather similar. This agrees with the experimental data.

With regard to the simple metal particles we have shown that the self-energy approach yields very good overall agreement with the full quantum-mechanical results for the complex polarizability. This leads us to an interesting new interpretation of a previously unidentified spectral feature at frequencies between the Mie resonance and the volume plasmon, namely a quasicollective excitation analogous to the multipole surface plasmon that is seen both theoretically and experimentally on all simple metal surfaces. Recent absorption spectra for large K clusters do indeed provide evidence for the fact that this mode also exists in small metal particles.

[1]R. Contini and J. M. Layet, Solid State Commun. **64**, 1179 (1987).

[2]S. Suto, K. D. Tsuei, E. W. Plummer, and E. Burstein, Phys. Rev. Lett. **63**, 2590 (1989); G. Lee, P. T. Sprunger, E. W. Plummer, and S. Suto, *ibid.* **67**, 3198 (1991).

[3]M. Rocca and U. Valbusa, Phys. Rev. Lett. **64**, 2398 (1990); M. Rocca, M. Lazzarino, and U. Valbusa, *ibid.* **67**, 3197 (1991); **69**, 2122 (1992); M. Rocca, F. Moresco, and U. Valbusa, Phys. Rev. B **45**, 1399 (1992).

[4]K. D. Tsuei, E. W. Plummer, and P. J. Feibelman, Phys. Rev. Lett. **63**, 2256 (1989).

[5]K. D. Tsuei, E. W. Plummer, A. Liebsch, K. Kempa, and P. Bakshi, Phys. Rev. Lett. **64**, 44 (1990); K. D. Tsuei, E. W. Plummer, A. Liebsch, E. Pehlke, K. Kempa, and P. Bakshi, Surf. Sci. **247**, 302 (1991).

[6]J. Harris and A. Griffin, Phys. Lett. **34A**, 51 (1971); F. Flores and F. Garcia-Moliner, Solid State Commun. **11**, 1295 (1972).

[7]P. J. Feibelman, Prog. Surf. Sci. **12**, 287 (1982); Phys. Rev. B **40**, 2752 (1989).

[8]For an excellent review, see U. Kreibig and L. Genzel, Surf. Sci. **156**, 678 (1985).

[9](a) K. P. Charlé, W. Schulze, and B. Winter, Z. Phys. D **12**, 471 (1989); (b) W. Harbich, S. Fedrigo, and J. Buttet, Chem. Phys. Lett. **195**, 613 (1992).

[10]J. Tiggesbäumker, L. Köller, H. O. Lutz, and K. H. Meiwes-Broer, Chem. Phys. Lett. **190**, 42 (1992).

[11]J. Tiggesbäumker, L. Köller, K. H. Meiwes-Broer, and A. Liebsch, Phys. Rev. A **48**, 1749 (1993).

[12]See: C. Bréchignac, Ph. Cahuzac, N. Kebaili, J. Leygnier, and A. Sarfati, Phys. Rev. Lett. **68**, 3916 (1992), and references therein.

[13]For a recent review, see V. V. Kresin, Phys. Rep. **220**, 1 (1992).

[14]D. Pines, *Elementary Excitations in Solids* (Benjamin, New York, 1963), p. 211.

[15]A. Zangwill and P. Soven, Phys. Rev. A **21**, 1561 (1980); M. J. Stott and E. Zaremba, *ibid.* **21**, 121 (1980); G. Mahan, *ibid.* **22**, 1780 (1980).

[16]W. Ekardt, Phys. Rev. B **31**, 6360 (1985).

[17]J. Tarriba and W. L. Mochán, Phys. Rev. B **46**, 12 902 (1992).

[18]P. J. Feibelman, Surf. Sci. **282**, 129 (1993).

[19]E. Lipparini and F. Pederiva, Z. Phys. D (to be published).

[20]E. Zaremba and W. Kohn, Phys. Rev. B **13**, 2270 (1976); B. N. J. Persson and E. Zaremba, *ibid.* **30**, 5669 (1984).

[21]P. Apell and C. Holmberg, Solid State Commun. **49**, 693 (1984).

[22]A. Liebsch, Phys. Rev. Lett. **71**, 145 (1993).

[23]B. N. J. Persson and E. Zaremba, Phys. Rev. B **31**, 1863 (1985).

[24]A. Liebsch, Phys. Rev. B **36**, 7378 (1987).

[25]K. Kempa and W. L. Schaich, Phys. Rev. B **37**, 6711 (1988); K. Kempa, A. Liebsch, and W. L. Schaich, *ibid.* **38**, 12 645 (1988).

[26]J. T. Lee and W. L. Schaich, Phys. Rev. B **44**, 13 010 (1991).

[27]A. Liebsch, G. V. Benemanskaya, and M. N. Lapushkin, Surf. Sci. (to be published).

[28]A. Liebsch, G. Hincelin, and T. López-Ríos, Phys. Rev. B **41**, 10 463 (1990).

[29]H. Ishida and A. Liebsch, Phys. Rev. B **45**, 6171 (1992).

[30]H. J. Hagemann, W. Gudat, and C. Kunz, J. Opt. Soc. Am. **65**, 742 (1975).

[31]P. Zacharias and K. L. Kliewer, Solid State Commun. **18**, 23 (1976).

[32]P. Apell and Å. Ljungbert, Solid State Commun. **44**, 1367 (1982).

[33]D. R. Snider and R. S. Sorbello, Phys. Rev. B **28**, 5702 (1983).

[34]E. Zaremba and B. N. J. Persson, Phys. Rev. B **35**, 596 (1987).

[35]W. Ekardt (private communication).

[36]M. A. Smithard, Solid State Commun. **14**, 407 (1974).

[37]J. Tiggesbäumker, L. Köller, and K. H. Meiwes-Broer (unpublished).

[38]W. Begemann, K. H. Meiwes-Broer, and H. O. Lutz, Phys. Rev. Lett. **56**, 2248 (1986).

[39]H. G. Liljenvall and A. G. Mathewson, J. Phys. C **3**, 5341 (1970).